The EMBO Journal (2012) 31, 4276–4288 | © 2012 European Molecular Biology Organization | All Rights Reserved 0261-4189/12
www.embojournal.org

THE EMBO JOURNAL

Hypothalamic AgRP-neurons control peripheral substrate utilization and nutrient partitioning

Aurélie Joly-Amado[1], Raphaël GP Denis[1], Julien Castel[1,2], Amélie Lacombe[1], Céline Cansell[1], Claude Rouch[1,2], Nadim Kassis[1,2], Julien Dairou[1], Patrice D Cani[3], Renée Ventura-Clapier[4], Alexandre Prola[4], Melissa Flamment[5,6], Fabienne Foufelle[5,6], Christophe Magnan[1] and Serge Luquet[1,2,*]

[1]Univ Paris Diderot, Sorbonne Paris Cité, Unité de Biologie Fonctionnelle et Adaptative, CNRS EAC 4413, Paris, France, [2]Centre National de la Recherche Scientifique-CNRS EAC 4413, Paris, France, [3]Université Catholique de Louvain, Louvain Drug Research Institute, Metabolism and Nutrition Research Group, Brussels, Belgium, [4]INSERM, UMR-S769, Univ Paris-Sud, Châtenay-Malabry, France, [5]INSERM, UMR-S 872, Centre de Recherche des Cordeliers, Paris, France and [6]Université Pierre et Marie Curie-Paris 6, Paris, France

Obesity-related diseases such as diabetes and dyslipidemia result from metabolic alterations including the defective conversion, storage and utilization of nutrients, but the central mechanisms that regulate this process of nutrient partitioning remain elusive. As positive regulators of feeding behaviour, agouti-related protein (AgRP) producing neurons are indispensible for the hypothalamic integration of energy balance. Here, we demonstrate a role for AgRP-neurons in the control of nutrient partitioning. We report that ablation of AgRP-neurons leads to a change in autonomic output onto liver, muscle and pancreas affecting the relative balance between lipids and carbohydrates metabolism. As a consequence, mice lacking AgRP-neurons become obese and hyperinsulinemic on regular chow but display reduced body weight gain and paradoxical improvement in glucose tolerance on high-fat diet. These results provide a direct demonstration of a role for AgRP-neurons in the coordination of efferent organ activity and nutrient partitioning, providing a mechanistic link between obesity and obesity-related disorders.

The EMBO Journal (2012) **31,** 4276–4288. doi:10.1038/emboj.2012.250; Published online 18 September 2012
Subject Categories: cellular metabolism; neuroscience
Keywords: diabetes; metabolism; obesity

Introduction

The last several decades have witnessed a pandemic expansion of pathologies related to high-fat and high-carbohydrate diets including obesity, diabetes, dyslipidemia and cardiovascular diseases—collectively referred to as metabolic syndrome. It is now evident that common obesity is polygenic and that although several genes (e.g., *Mc4r*, *Bdnf*, *Fto*) have been identified as causing rare monogenic obesity (Walley *et al*, 2009), metabolic syndrome results from complex genetic interactions affecting susceptibility to obesity and the radical environmental changes that have occurred during the last century. Moreover, it has become evident that obesity-related metabolic complications are not solely caused by excessive nutrient intake, but also involve the inappropriate conversion, storage and utilization of nutrients.

In the brain, the arcuate nucleus (ARC) of the hypothalamus contains at least two crucial populations of neurons that continuously monitor signals reflecting energy status and promote the appropriate behavioural and metabolic responses to changes in nutritional availability and demand (Elmquist *et al*, 1999; Schwartz *et al*, 2000; Cone, 2005; Morton *et al*, 2006; Ahima and Antwi, 2008). Neurons making pro-opiomelanocortin (POMC) decrease food intake and increase energy expenditure through activation of melanocortin receptors (MCR) via the release of α-melanocyte stimulating hormone (α-MSH). Activity of neighbouring neurons expressing the orexigenic neuropeptides, agouti-related protein (AgRP) and neuropeptide Y (NPY) (AgRP-neurons) increase feeding by opposing the anorexigenic actions of the neighbouring POMC neurons (Horvath *et al*, 1992, 2004; Cowley *et al*, 2001; Pinto *et al*, 2004), in part through the release of AgRP, a competitive inhibitor of MCRs (Saper *et al*, 2002; Cone, 2005; Morton *et al*, 2006). Beside the consensus view that AgRP-neurons exert their positive action on feeding behaviour primarily by opposing melanocortin signalling (Saper *et al*, 2002; Cone, 2005; Morton *et al*, 2006), it has been recently demonstrated that the action of AgRP-neurons on energy balance regulation involves their release of γ-aminobutyric acid (GABA) in brain regions where the melanocortin signalling pathway is not active (Wu *et al*, 2008, 2009; Dietrich and Horvath, 2009; Wu and Palmiter, 2011). Moreover, selective activation of AgRP-neurons using optogenetics demonstrated that inhibition of the α-MSH signalling cascade is not required for AgRP-neurons to initiate the complex behavioural sequence that leads to food intake (Aponte *et al*, 2011). It is therefore becoming evident that the regulation of energy balance by AgRP-neurons involves melanocortin-independent signalling outside of the hypothalamus. Interestingly, AgRP-neurons send dense projections to preganglionic structures such as the paraventricular nucleus (PVN), that directly regulate autonomic nervous system (ANS) outflow to peripheral tissues (Broberger *et al*, 1998; Broberger and Hokfelt, 2001; Broberger, 2005). We therefore hypothesized that the action of AgRP-neurons on energy balance might extend beyond the acute control of food intake.

*Corresponding author. Biologie Fonctionnelle et Adaptative BFA, EAC 4413, Univ Paris Diderot, Sorbonne Paris Cité, 4 rue Marie-Andrée Lagroua Weill-Hallé, Bâtiment Buffon, Paris 75013, France.
Tel.: +33 1 57 27 77 93; Fax: +33 1 57 27 77 96;
E-mail: serge.luquet@univ-paris-diderot.fr

Received: 28 March 2012; accepted: 16 August 2012; published online: 18 September 2012

In order to explore this hypothesis, we used a model of neonatal depletion of AgRP-neurons. Acute ablation of AgRP-neurons in adult animals leads to anorexia, whereas neonatal depletion is tolerated (Bewick *et al*, 2005; Gropp *et al*, 2005; Luquet *et al*, 2005; Xu *et al*, 2005). We first hypothesized that a network-based compensatory mechanism allowed survival in mice lacking AgRP-neuron from birth. However, a recent study suggests that the starvation that results from adult ablation involves the acute loss of GABAergic input from AgRP-neurons and consequent hyperactivity of the parabrachial nucleus (PBN) (Dietrich and Horvath, 2009; Wu *et al*, 2009; Wu and Palmiter, 2011). AgRP neurocircuitry is not fully formed in mice until day 21 after birth (Bouret *et al*, 2004; Nilsson *et al*, 2005). Thus neonatal ablation, performed at days 3–6 after birth, is unlikely to create PBN hyperactivity since the processes arising from AgRP-neurons have not yet reached that structure. In that view, mice lacking AgRP-neurons provide a good model to define new function of this neurocircuitry in a context where acute starvation is not potentially masking subtle phenotypes.

Using this we have unravelled a new role for these neurons in orchestrating the fate of a nutrient once ingested by controlling the peripheral conversion, storage and utilization of nutrients. This new function of AgRP-neurons comes in addition to their well-known effects on the regulation of food intake. Here we report that, in addition to affecting food intake, the ablation of AgRP-neurons alters inter-organ communication and redirects peripheral nutrient utilization towards increased fat, versus carbohydrate, oxidation. This study highlights a key function of AgRP-neurons as central coordinators of peripheral energy partitioning and offers new opportunities for the treatment of obesity-related pathologies that compose the metabolic syndrome.

Results

Mice lacking AgRP-neurons become obese on a regular chow diet

To specifically address the role of AgRP-neurons in the central coordination of peripheral organ activity, we selectively ablated AgRP-expressing neurons in mice at the neonatal stage. Briefly, mice carrying the gene encoding the human diphtheria toxin (DT) receptor placed downstream of the regulatory sequence of *Agrp* were injected with DT during the first week after birth (AgRP-ablated mice) as described previously (Luquet *et al*, 2005). Control mice of the same genotype were injected with saline (naive mice).

Considering the known orexigenic function of AgRP-neurons one might expect AgRP-ablated mice to be hypophagic and lean. Indeed, mice lacking AgRP-neurons mice show a blunted feeding response to both peripherally injected ghrelin (Figure 1A) and to a 24-h fast (Figure 1B) as observed previously (Luquet *et al*, 2007). Unexpectedly however, AgRP-ablated mice became obese by ~3 months of age on a regular chow diet (RCD) (Figure 1C). Although food intake was identical between naive and AgRP-ablated mice when tested at multiple ages (Figure 1D), feeding efficiency (weight gain/kcal consumed) was significantly higher in AgRP-ablated mice (Figure 1E), suggesting that mechanisms other than caloric consumption were responsible for the weight gain. Adipose tissue expansion accounted for the entire body weight gain in AgRP-ablated mice, and most fat

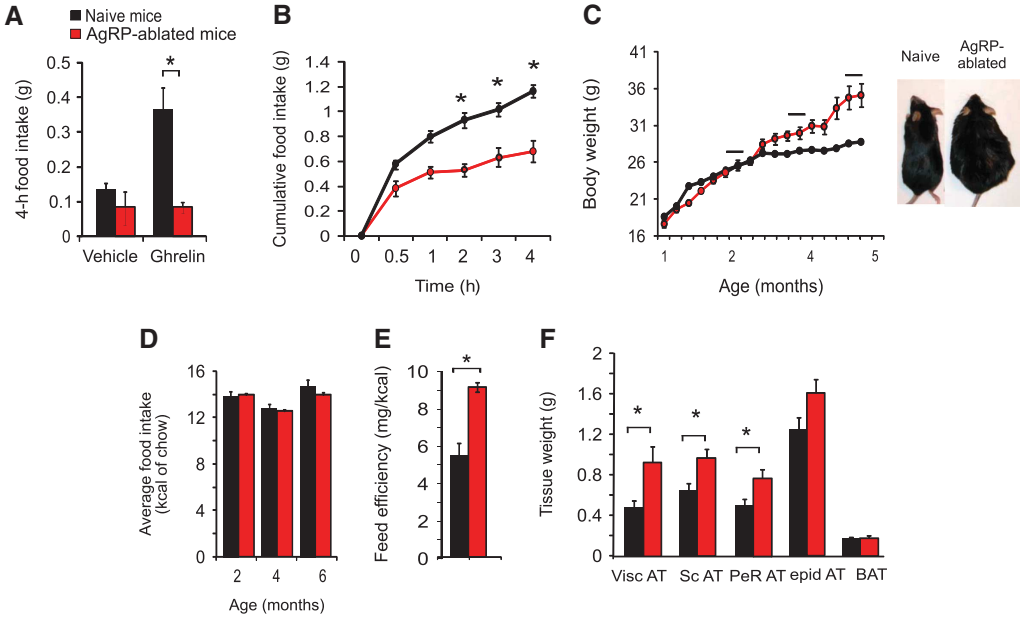

Figure 1 Mice lacking AgRP-neurons become obese on RCD. In all, 4-h feeding response after an intraperitoneal (IP) injection of saline or ghrelin (500 μg/kg) (**A**), or after a 24-h fast (**B**) in naive (black bars and circles) and AgRP-ablated mice (red bars and circles). ($n = 6$–9 in each group). Average body weight in naive (black circles) and AgRP-ablated mice (red circles) fed on RCD ($n = 6$–7 in each group) (**C**). Average food intake in kcal of chow was recorded at several time points at age 2, 4 and 6 months (black bar in Figure 1C) ($n = 6$–7 in each group) (**D**). Feed efficiency is presented as mg of body weight gain/kcal consumed during a 4-month period (**E**). Adipose tissue weight after a 24-h fast (Visc AT: visceral adipose tissue, Sc AT: subcutaneous adipose tissue, Perirenal AT: perirenal adipose tissue, epid AT: epididymal adipose tissue) (**F**). Displayed values are mean values ± s.e.m. $^*P < 0.05$ ($n = 6$–7 in each group).

depots were affected (Figure 1F), while other peripheral organs appeared grossly normal and did not differ significantly by weight (data not shown).

A metabolic shift towards lipid oxidation is associated with obesity in AgRP-ablated mice

We next assessed metabolic efficiency using indirect calorimetry in obese AgRP-ablated mice and lean naive mice. Obese AgRP-ablated mice did not display a decrease, but rather a slight increase in both O_2 consumption (Supplementary Figure 1a) and energy expenditure (Figure 2A; Supplementary Figure 1b) when normalized to lean body mass (LBM) measured by nuclear magnetic resonance (NMR) (Butler and Kozak, 2010). These findings rule out that reduced metabolic efficiency is the primary contributor to the obese phenotype. However, total dark-phase locomotor activity (Figure 2B) as well as body temperature (Figure 2C) were substantially decreased in obese AgRP-ablated mice and may thus contribute to the body weight gain.

In addition, control experiments including *ob/ob* mice and AgRP-ablated mice at a comparable level of obesity clearly showed a positive energy balance in *ob/ob* mice (consumed/expended) that was about twice that of both naive and AgRP-ablated mice (Supplementary Figure 1d).

Respiratory quotient (RQ) is the ratio of vCO_2/vO_2 and provides an indication of the nature of the substrate being used by an organism (i.e., RQ = 1 for glucose utilization RQ = 0.7 for lipid utilization). RQ profiles acquired over several days demonstrated a significant decrease that was repeatedly observed in AgRP-ablated mice relative to naive controls at the entry of the dark period (Figure 2D). This decrease was not associated with a change in food intake or feeding rhythm, which were identical across groups (Supplementary Figure 1c).

Interestingly, the entry of the dark cycle in *ad libitum* fed rodents corresponds to the point when they are hungriest, energy levels lowest and activity of AgRP-neurons is likely to be highest (Cowley *et al*, 2003). In addition, this decrease in RQ at the entry of the dark period was a specific feature of AgRP-ablated mice. Indeed, when acquired simultaneously, the RQ profiles of AgRP-ablated mice and o*b/ob* was found to significantly differ at the entry of the dark cycle (Supplementary Figure 2a).

Finally, during a 24-h fast, naive and AgRP-ablated mice were equally able to shift onto pure oxidative metabolism (with RQ falling to 0.7), but the rebound period was characterized by a sustained decrease in RQ in AgRP-ablated mice, again indicative of a shift towards oxidative

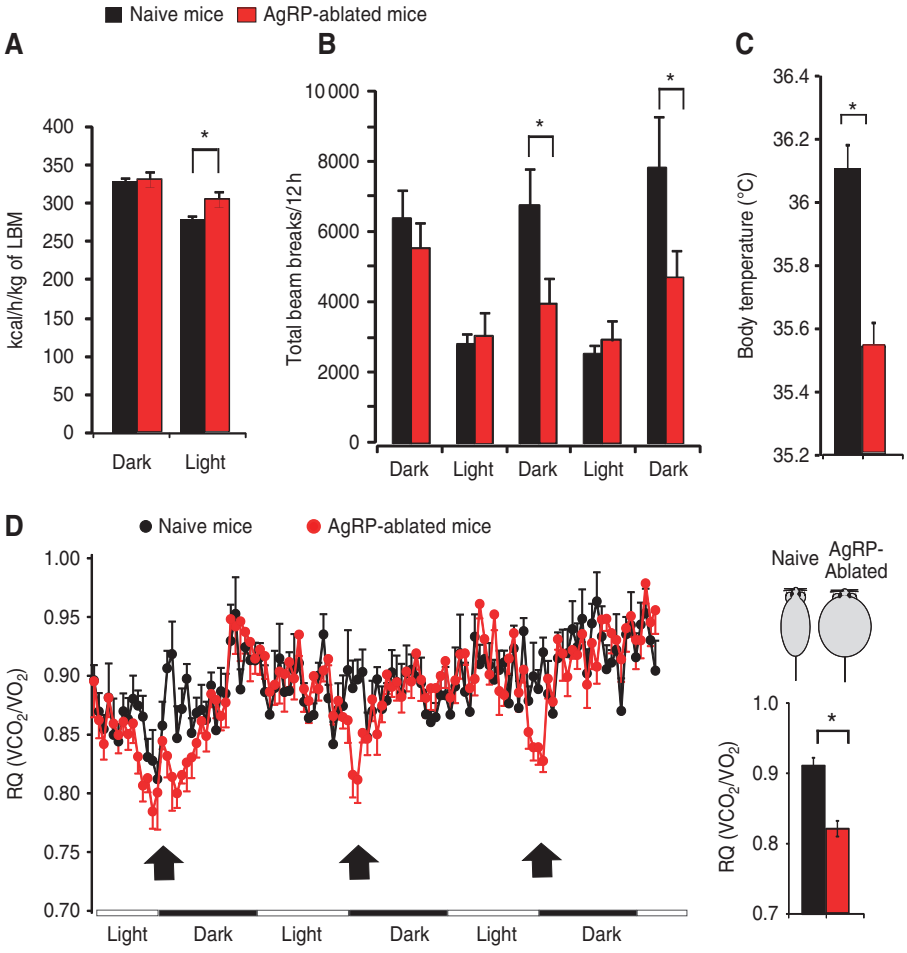

Figure 2 Metabolic shift towards lipid oxidation and modified energy expenditure is associated with obesity in mice lacking AgRP-neurons. Energy expenditure (kcal/h/kg of LBM) (**A**), total locomotor activity (**B**), average daily subcutaneous temperature (**C**) (*$P<0.05$ using linear regression model), daily variation of RQ analysis (VCO_2/VO_2) and average value for RQ (histogram) at the time period indicated with an arrow (**D**) (Figure 2C) (*$P<0.05$ using repeated measure ANOVA). Data were acquired on 6-month-old lean naive animals (black bars and black circles) and obese AgRP-ablated (red bar and red circles) ($n = 6$ in each group). Displayed values are mean values ± s.e.m. *$P<0.05$.

metabolism (Supplementary Figure 2b). Therefore, AgRP-neurons appear to play a role in the regulation of nutrient utilization independent from their effects on food intake.

AgRP-ablated mice display a tissue-specific modulation of sympathetic nervous system outflow that precedes the onset of obesity

This shift towards lipid utilization suggests the possibility for modified nutrient partitioning, a process that requires the coordinated dialogue between organs including post-prandial insulin release from pancreas, nutrient conversion and storage in the liver and adipose tissue, and glucose/lipid utilization in muscle (Nogueiras *et al*, 2007, 2010; Yamada *et al*, 2008). Nutrient partitioning relies on the ability of the brain to orchestrate peripheral organ activity through the modulation of ANS output. We therefore explored the hypothesis that a change in ANS-mediated regulation of peripheral organ activity contributed to the increase in lipid utilization and obesity in AgRP-ablated mice.

ANS output is centrally determined at the level of preganglionic structures such as the PVN, which receives dense projections from AgRP-neurons (Cowley *et al*, 1999) and increased AgRP-neuron activity during energy deprivation leads to reductions in postsynaptic neuron activity (Cowley *et al*, 1999). As expected, the lack of AgRP-neurons led to a reduction in c-Fos-positive nuclei in the ARC following a 48-h fast (Figure 3A). Furthermore, whereas naive animals displayed few c-fos-positive neurons in the PVN, abundant c-Fos-positive cells were found in the PVN of mice lacking AgRP-neurons (Figure 3A).

To directly test whether sympathetic nervous system (SNS) outflow onto peripheral tissue is affected by the loss of AgRP-neurons, we used the synthesis inhibition method (Brodie *et al*, 1966) to measure the catecholamine turnover rate (cTR) in various tissues, and prior to the onset of obesity in AgRP-ablated mice. Treatment with α-methyl-p-tyrosine (α-MPT) blocked norepinephrine (NE) synthesis (Figure 3B–E) and the slope of this decrease in tissue NE content was multiplied by the initial concentration to yield cTR, an indirect readout of SNS outflow. In mice lacking AgRP-neurons, cTR was significantly decreased in pancreas (Figure 3B), liver (Figure 3C) and the fast-glycolytic muscle extensor digitorum longus (EDL) (Figure 3D). On the contrary, the slow-oxidative soleus muscle (Sol) displayed the opposite phenotype with an increased cTR (Figure 3E). The hindbrain and hypothalamus were also evaluated as control tissues and did not show differences in NE cTR (Supplementary Figure 3a and b). Interestingly, in AgRP-ablated mice we found no changes in cTR in white adipose depots (Supplementary Figure 4a and b) but with a non-significant trend towards a decrease in brown adipose tissue (BAT) (Supplementary Figure 4c). Moreover, we found that fasting induced release of free fatty acid (FFA) is similar in naive and AgRP-ablated mice (Supplementary Figure 5), suggesting that adrenergic-mediated release of FFA by the adipose tissue was unaltered in AgRP-ablated mice.

β-Cell insulin release depends on the reciprocal activities of the sympathetic and parasympathetic nervous systems (PNS) (Rohner-Jeanrenaud *et al*, 1983). PNS-mediated activation of muscarinic receptors onto β-cells increases insulin release while SNS-mediated activation of α2 adrenergic receptors (α2AR) has the opposite effect (Ahren *et al*, 1986; Ahren, 2000).

Prior to any change in body weight, when AgRP-ablated and naive mice are still comparably lean, plasma insulin was significantly higher in AgRP-ablated mice (Figure 3F).

In order to evaluate if the decreased SNS outflow is a primary contributor of hyperinsulinaemia, we attempted to pharmacologically correct this phenotype in AgRP-ablated mice prior to, and after the establishment of obesity. We found indeed that injection of the α2AR agonist clonidine normalized plasma insulin levels in AgRP-ablated mice in both lean (Figure 3F) and obese condition (Figure 3G). These results strongly suggest that a change in SNS outflow was instrumental in the phenotype of AgRP-ablated mice both before and after the onset of obesity. Note that the injection of a muscarinic receptor antagonist atropine methyl bromide had no effect (data not shown). These results strongly support our hypothesis that increased plasma insulin levels were an early consequence of decreased SNS outflow (but not PNS) onto pancreas and not simply a secondary adaptation to obesity.

AgRP-ablated mice display enhanced liver lipid production and peripheral utilization

The decrease in RQ we observed in AgRP-ablated mice indicates a preferential utilization of lipid-substrate (Figure 2D; Supplementary Figure 2). The liver plays an integral role in nutrient conversion and can actively transform carbohydrate into lipid (Porter and Brand, 1993), thereby providing a potentially major source of triglyceride (TG) in AgRP-ablated mice. Moreover, the decrease in sympathetic liver outflow should result in reduced glucose export while favouring lipid synthesis (Nonogaki, 2000). Indeed, obese AgRP-ablated mice displayed higher TG content in the liver as determined by both oil red O staining (data not shown) and biochemical analysis (Figure 4A). Plasma TG were more abundantly distributed in liver-born very low-density lipoprotein (VLDL) than in low-density lipoprotein (LDL) in AgRP-ablated mice compared with naive mice (Figure 4B). Further, plasma TG levels were elevated in AgRP-ablated mice soon after the post-prandial period but normalized following 3-h food deprivation, indicating that TG were actively used as a source of energy (Figure 4C). This suggests a more active synthesis of TG-rich particles by the liver and an enhanced utilization of TG by peripheral tissue. Enhanced lipogenic activity in the liver was supported by qRT–PCR analysis, which revealed an upregulation of mRNA encoding proteins involved in the lipogenic pathway, such as the sterol regulatory element binding protein 1c (SREBP-1c), glucokinase (GK) and the stearoyl-CoA desaturase 1 (SCD1) (Figure 4D); whereas others remained unchanged (Figure 4D; Supplementary Figure 6).

In order to directly challenge the ability of obese AgRP-ablated mice to dispose of TG, we administered an oral charge of lipids (olive oil 15 μl/g BW) (as described by Kim *et al*, 2007). After oral TG gavage (at $t = 0$), AgRP-ablated and naive mice displayed a similar plasma TG excursion and clearance (Figure 4E). These observations show that, despite their obesity, mice lacking AgRP-neurons retained the ability to store TG. Both free plasma glycerol and FFA, the products of TG breakdown, were significantly increased in mice lacking AgRP-neurons (Figure 4F and G). The latter result could point towards an enhanced TG breakdown that would be

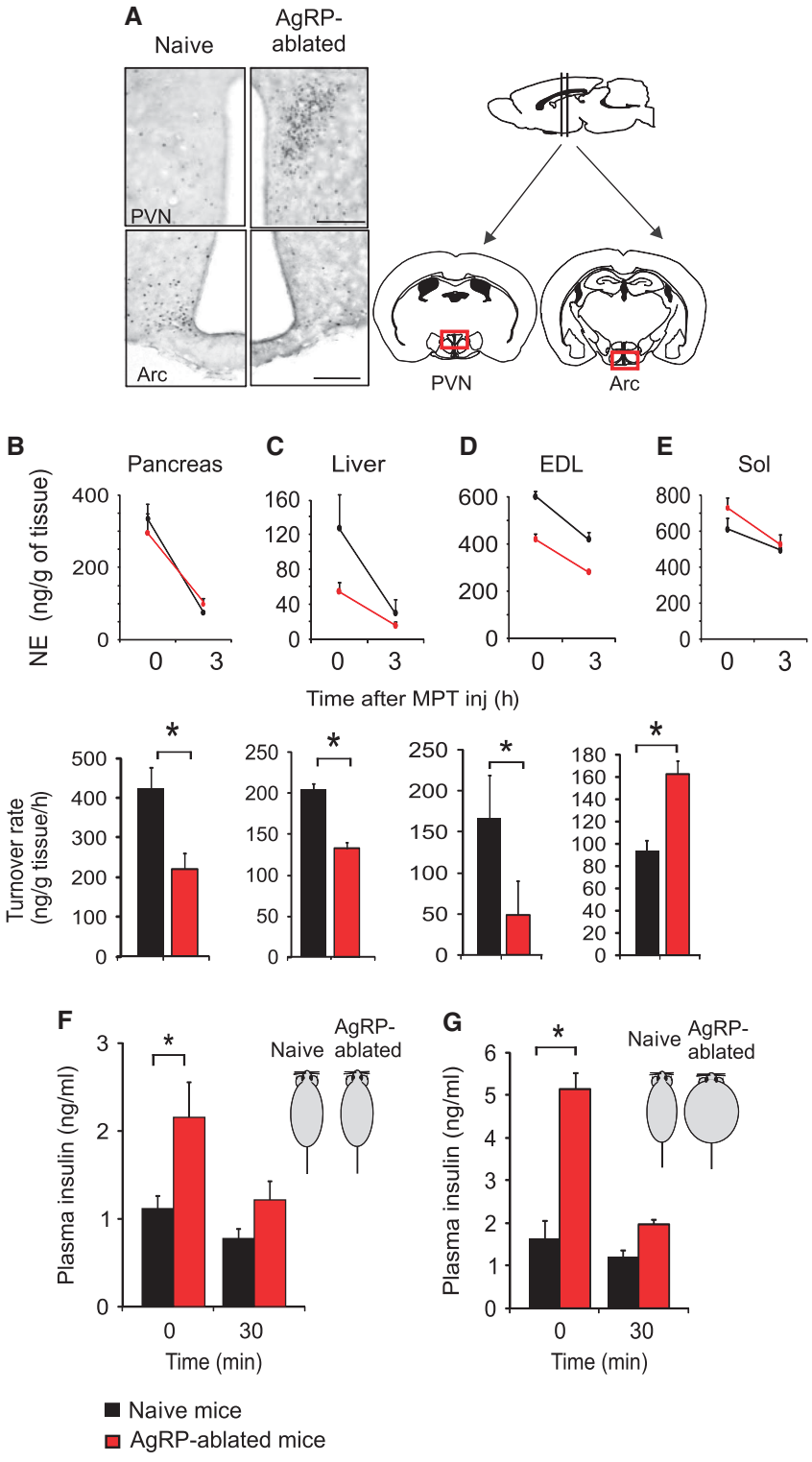

Figure 3 The lack of AgRP-neurons is associated with a change in the distribution of SNS output onto peripheral tissues that precedes obesity. Representative immunohistochemistry for c-fos in naive (left) and AgRP-ablated mice (right) after a 48-h fast in the ARC and the PVN of the hypothalamus. Scale bar = 100 μm (**A**). Representative decrease in tissue NE content after α-MPT injection (upper panel) and, turnover rate (TR) (lower panel in histogram) (**B**–**E**) were determined on pancreas (**B**), liver (**C**), white glycolytic muscle EDL (**D**) and red oxidative muscle soleus (Sol) (**E**). Plasma insulin levels after 5-h food deprivation were measured prior (time = 0) and 30 min after an intraperitoneal injection of the α2-adrenergic receptor agonist clonidine (50 nmol/kg of body weight) (**F**, **G**). (**A**–**F**) All measurements were acquired on lean naive (black bar and black circles) and lean AgRP-ablated mice (red bar and red circles) at a time point that preceded obesity ($n = 5$–8 in each group) while Figure 3G present plasma insulin change after clonidine injection in lean naive and obese AgRP-ablated mice after obesity has established (**G**) ($n = 6$–8 in each group). Displayed values are mean values ± s.e.m. $^*P < 0.05$.

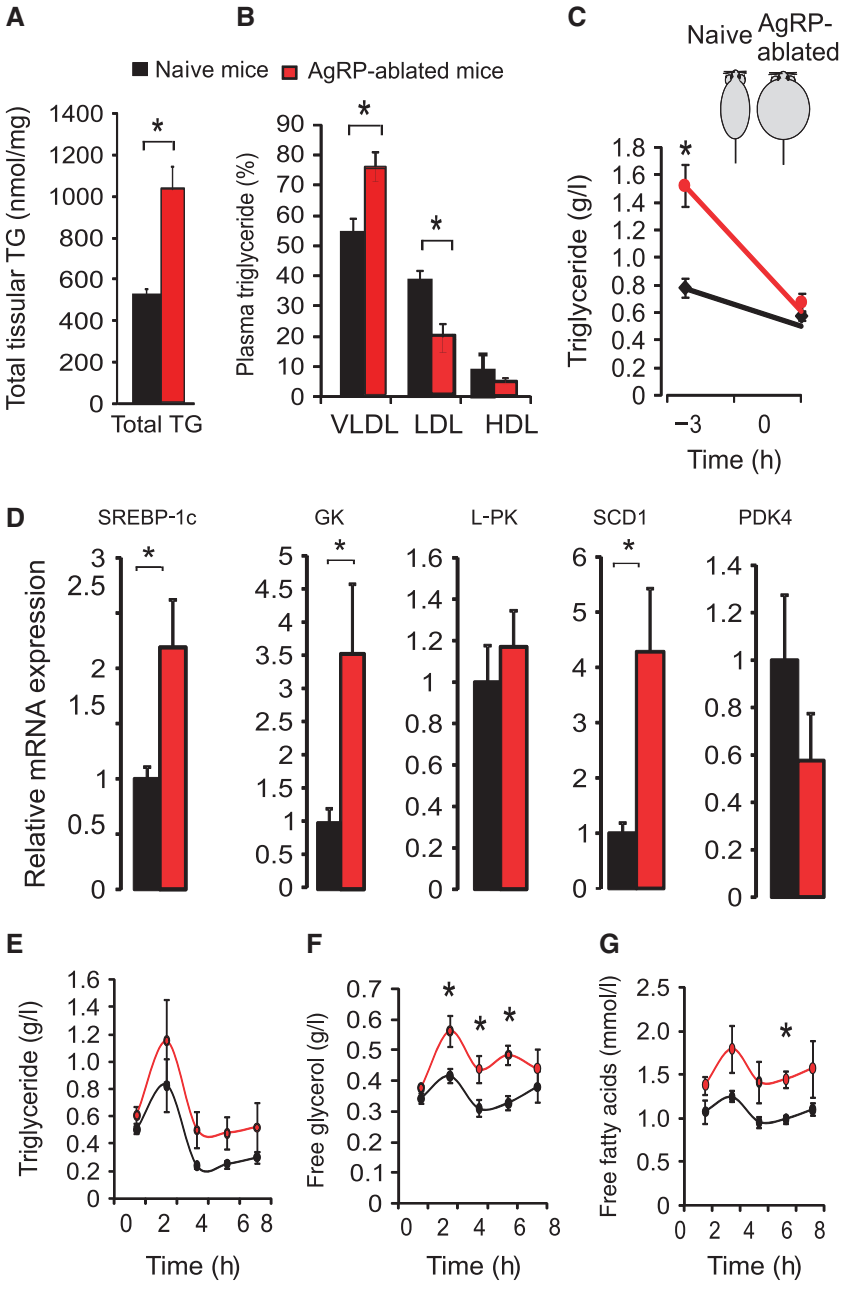

Figure 4 The lack of AgRP-neurons conveys an increased hepatic liver lipid production associated with increased lipid utilization. Liver TG quantification (total TG) (**A**) and plasma TG distribution (**B**) (in %) in circulating VLDL, LDL, HDL, respectively, in lean naive mice (black bar) compared with obese AgRP-ablated mice (red bar) after a 24-h fast. Plasma TG content prior (time = −3 h) and after (time = 0) a 3-h food deprivation (**C**) at the beginning of the light period on lean naive (black circles) and obese-ablated mice (red circles). Total liver RNA was extracted and analysed by qRT–PCR for SREBP-1c, GK, L-PK (L-pyruvate kinase), SCD1 (stearoyl CoA desaturase 1) and PDK4 (pyruvate dehydrogenase isozyme kinase 4) after a 24-h fast (**D**). Plasma TG (g/l) (**E**), free glycerol (g/l) (**F**) and FFAs (mmol/l) (**G**) in lean naive mice (blacks circles) and obese AgRP-ablated mice (red circles) after an oral charge of lipid (15 μl/g of body weight of olive oil) at time = 0. Displayed values are mean values ± s.e.m. *$P<0.05$.

consistent with enhanced utilization of TG in the periphery. However, this result could also be explained by a decrease utilization of FFA and glycerol.

Taken together, these results suggest that AgRP-neurons contribute to the equilibrium between carbohydrate and lipid partitioning, partly through the control of liver nutrient conversion, together with peripheral storage and utilization of lipids.

Loss of AgRP-neurons conveys a preference for lipid substrate utilization in muscle mitochondria

Sympathetic outflow is an important determinant of muscle metabolism (Haque *et al*, 1999; Shiuchi *et al*, 2009). We reasoned that changes in cTR (Figure 3D and E), which oppositely affected glycolytic and oxidative muscle, may produce changes in the oxidative capability of these muscles. Loss of AgRP-neurons did not lead to significant changes

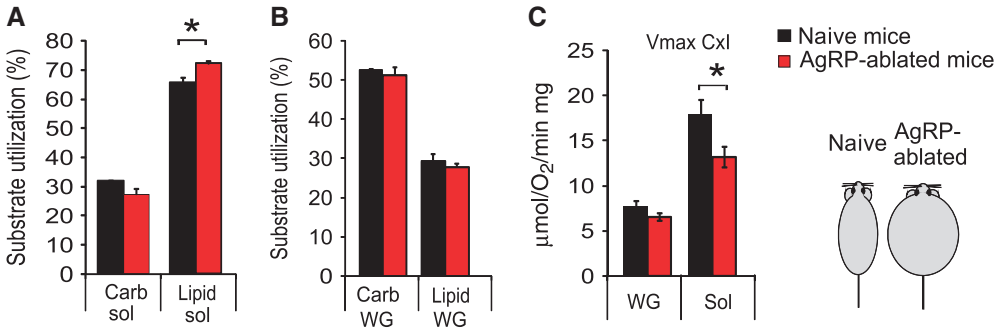

Figure 5 Ablation of AgRP-neurons leads to an increase in lipid-substrate utilization in oxidative muscle mitochondria. Mitochondrial respiration rates measured in permeabilized fibres for carbohydrate substrate (pyruvate) or lipid utilization presented in percentage of the maximal respiration measured with glutamate in soleus muscle (sol) (**A**) and white fast gastrocnemius (WG) (**B**) in lean naive mice (black bar) and obese AgRP-ablated mice (red bar) fed a RCD. Mitochondrial respiration rates with complex I substrates (**C**) in white gastrocnemius (WG) and soleus muscles (Sol) ($n = 6$ in each group). Displayed values are mean values ± s.e.m. $^*P < 0.05$.

in expression of genes involved in the transport of lipids or intracellular lipid handling (not shown). We therefore directly measured mitochondrial respiration rates and substrate preference *in situ* using permeabilized isolated fibres and found that AgRP-ablated mice displayed enhanced capacity for lipid-substrate utilization in oxidative soleus muscle while carbohydrate utilization remained unaffected (Figure 5A). This change was associated with a decrease in the maximal OXPHOS complex I respiration rate (Figure 5C). These changes were specific to the soleus muscle, as no changes were observed in respiratory kinetics or substrate preference in white gastrocnemious (a typical 'fast glycolytic muscle') (Figure 5B and C). It is unlikely that such changes in respiration were merely due to mitochondrial depletion, as respiration measured in respiratory complex II, I + II and IV remained unaltered (Supplementary Tables 1–3). These results show that the increase in NE cTR onto soleus muscle was indeed associated with an enhanced oxidative capability for lipids, and may thereby contribute to the shift towards oxidative metabolism evidenced by the RQ measurements in AgRP-ablated mice.

A high-fat diet provides paradoxical benefits for mice lacking AgRP-neurons

Because mice lacking AgRP-neurons favoured lipid over carbohydrate metabolism, we hypothesized that they may be protected against the deleterious effects induced by a high-fat diet (HFD). We shifted groups of naive and obese AgRP-ablated mice from a RCD to an HFD (22.5% fat compared with 4% in RCD). After 6 months on an HFD, naive and AgRP-ablated mice reached a similar degree of adiposity. However, AgRP-ablated mice showed a normalization of feeding efficiency and a smaller gain in fat mass relative to naive animals (Figure 6A and B).

HFD resulted in a significant increase in blood glucose in naive mice (measured after a 5-h fast), whereas it remained unchanged in AgRP-ablated mice (Figure 6C). The same cohorts of naive and AgRP-ablated mice were subjected to a glucose tolerance test prior to, and after, HFD. Strikingly, whereas glucose clearance was equivalent between naive and AgRP-ablated mice on RCD (Figure 6D), HFD actually improved the ability of AgRP-ablated mice to dispose of glucose and led to a reduction in plasma insulin levels (Figure 6E and F). Collectively, these data indicate that HFD provided a paradoxical benefit on both glucose tolerance and insulin sensitivity in AgRP-ablated mice, presumably due to their preference for storing and using lipids.

Chronic $GABA_A$-receptor agonist treatment normalizes the phenotype of AgRP-ablated mice

The antagonistic action of AgRP on hypothalamic melanocortin signalling is one important part of the process by which these neurons regulate energy balance (Saper *et al*, 2002; Cone, 2005). However, AgRP-neurons also make GABA (Horvath *et al*, 1997) and it was recently shown that melanocortin-independent mechanisms, involving GABA release from AgRP-neurons also contribute to the regulation of energy balance (Wu *et al*, 2008; Dietrich and Horvath, 2009; Aponte *et al*, 2011; Wu and Palmiter, 2011). Along that line, we found that intracerebroventricular (ICV) injection of a low dose of AgRP peptide (0.1 nmol) produced a similar increase in feeding in both naive and AgRP-ablated mice, suggesting that loss of AgRP-neurons did not lead to a hypersensitivity of AgRP that could have resulted from the overall increase in the melanocortin system activity (not shown). We therefore attempted to pharmacologically rescue the phenotype of AgRP-ablated mice by chronically increasing GABA signalling, a strategy similar to that used by Wu *et al* (2009). Obese AgRP-ablated and lean naive mice were implanted with subcutaneous Alzet minipumps containing bretazenil (a $GABA_A$ receptor partial agonist). At the onset of treatment, AgRP-ablated mice displayed a RQ that was significantly lower than naive control mice at the entry of the dark cycle (Figure 7A) (as previously observed (Figure 2D)). However, following chronic bretazenil treatment, the RQ profile was no longer different between the groups (Figure 7B). Thus, increasing $GABA_A$ receptor activation normalized the ratio of fat to carbohydrate metabolism in AgRP-ablated mice.

Consistent with a shift in nutrient storage and utilization, bretazenil also caused a significant decrease in body fat content, selectively in AgRP-ablated mice that, importantly, reversed once the treatment was discontinued (Figure 7C). In addition, during bretazenil treatment body temperature was no longer decreased in AgRP-ablated mice (Figure 7D). Importantly, we could show that Bretazenil action onto body fat store was specific to the obesity displayed by AgRP-ablated mice. Indeed, subcutaneous replacement of bretazenil in obese *ob/ob* mice resulted in body weight gained

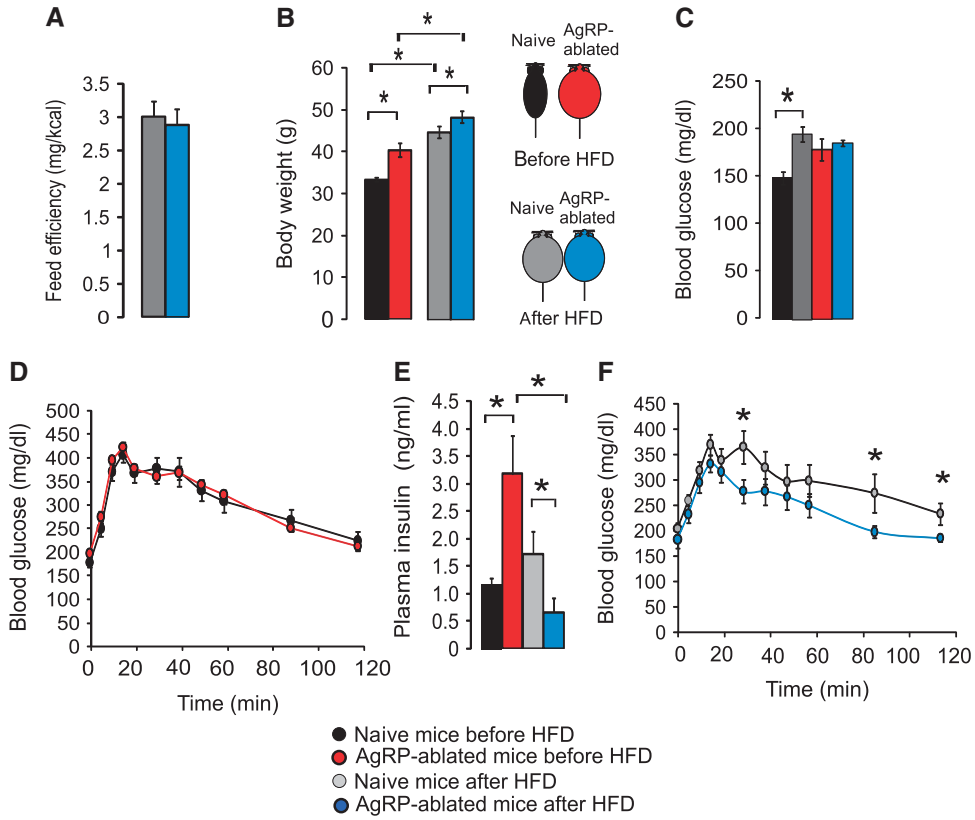

Figure 6 Lack of AgRP-neurons is associated with resistance to high-fat feeding. Feed efficiency as mg of body weight gain/kcal consumed calculated during a 2-month period during an HFD regimen (**A**), final body weight (**B**), blood glucose (mg/dl) after a 5-h food deprivation (**C**) and after an oral charge of glucose (3 g/kg) (**D**, **F**) and plasma insulin (ng/ml) (**E**), in naive mice (black and grey bars) and obese AgRP-ablated mice (red and blue bars). Data were acquired on the same group of animals fed a RCD before HFD regimen (black and red bars), and after a 6-month HFD regimen (grey and blue) ($n = 7$–8 in each group). Displayed values are mean values ± s.e.m. $^*P < 0.05$.

but no loss in body fat while inducing a small but significant decrease in adiposity selectively in obese AgRP-ablated mice (Supplementary Figure 9)

These results suggest that GABA may be the crucial signalling molecule by which AgRP-neurons control peripheral nutrient partitioning and substrate utilization.

Discussion

The metabolic syndrome represents a collection of risk factors for cardiovascular diseases that encompass components of obesity such as hypertension, dyslipidemia and diabetes (Eckel *et al*, 2005; Reaven, 2006). Despite the dangers and increasing prevalence of the metabolic syndrome, effective and safe treatments to stop its spread remain unavailable. Understanding the mechanisms by which the brain controls peripheral nutrient partitioning may prove essential to achieving a clinical breakthrough.

We report here that the selective destruction of AgRP-neurons leads to remarkable coordinated changes in ANS output onto efferent organs, characterized by a decrease in sympathetic activity in pancreas, liver and glycolytic muscle, and an increase in sympathetic activity onto oxidative muscle (Figure 3). This results in a switch in peripheral substrate utilization towards lipids (Figures 2 and 4) that is enhanced by a synergistic increase in liver TG synthesis and lipid oxidation capabilities in muscle mitochondria (Figures 5 and 8). As a consequence, AgRP-ablated mice show a significant increase in feeding efficiency (weight gain/kcal consumed) and become obese and hyperinsulinemic on chow diet (Figures 1 and 3). However, when placed on an HFD, these animals display reduced body weight gain and a paradoxical improvement in glucose tolerance and insulin sensitivity (Figure 6). Importantly, we were able to recapitulate these results in animals that were exposed to HFD since the weaning period, prior to any body weight difference. In these conditions, AgRP-ablated mice had growth curves similar to controls (Supplementary Figure 7a and d) but displayed increased locomotor activity and oxygen consumption (Supplementary Figure 7b–d), decreased RQ (Supplementary Figure 7e) and improved glucose clearance (Supplementary Figure 7f). These data provide further evidence that, even at comparable body weight, the imbalance between carbohydrate and fat partitioning subsequent to AgRP-neurons ablation allows better protection against HFD whereas it is presumably instrumental in body weight gain on a RCD.

Central circuits that control food intake also control peripheral nutrient partitioning

If one considers only the canonical antagonistic action of AgRP-neurons on the melanocortin signalling pathway, the predicted consequences of AgRP-neurons depletion are reduced feeding and body weight. Consistent with that view, the loss of AgRP-neurons is associated with a blunted feeding

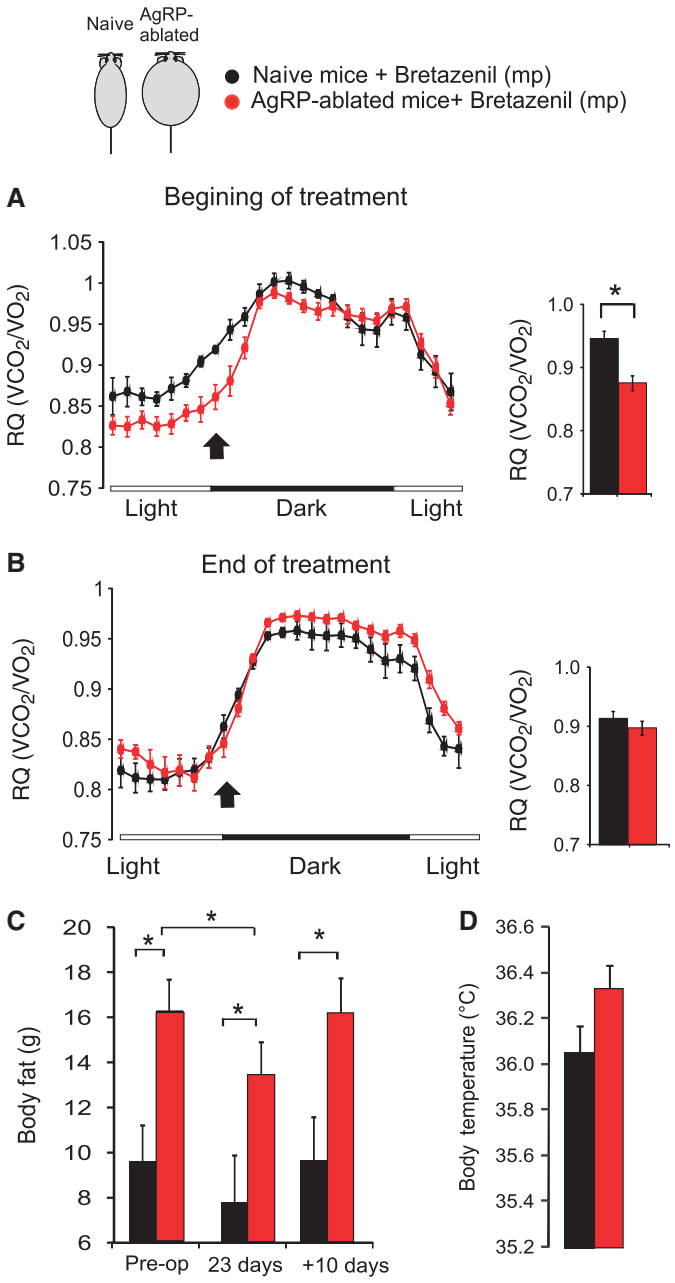

Figure 7 Chronic $GABA_A$-receptor agonist treatment normalizes the phenotype of AgRP-ablated mice. Representative distribution of RQ (VCO_2/VO_2) acquired by indirect calorimetry on the course of several days in naive (black circles) and obese AgRP-ablated mice (red circles) implanted with subcutaneous osmotic minipumps (mp) delivering the $GABA_A$ receptor partial agonist, bretazenil (0.25 μl/h; 3 mg/ml) (**A**, **B**). Data are presented as an average of 2 (**A**) or 3 (**B**) consecutive days acquired at the beginning (**A**) or during (**B**) the treatment. Average RQ value at the entry of the dark cycle, at a time indicated with an arrow, are presented as histogram (*$P<0.05$ using repeated measure ANOVA). Body fat content acquired by NMR in (**C**) on naive (black bars) and obese AgRP-ablated mice (red bars) prior to mp implantation (pre-op), during bretazenil delivery (at day = 23) or 10 days after the mp have run out ($n = 5$–7 in each group). Average daily subcutaneous temperature collected on 3 consecutive days during bretazenil treatment (**D**). Displayed values are mean values ± s.e.m. *$P<0.05$.

response to a fast or peripherally injected ghrelin (Luquet *et al*, 2007) (Figure 1A and B), an output that is recapitulated following the acute pharmacological inhibition of AgRP-neurons *in vivo* (Krashes *et al*, 2011). Despite these phenotypes however, we find that destruction of AgRP-neurons in pups leads to adult-onset obesity. Furthermore, this obesity is not due to increased caloric intake but rather involves a shift in substrate utilization due to simultaneous metabolic changes in a number of peripheral tissues. In this regard, the peripheral consequences of AgRP-neurons ablation present similarities with those observed after central MCR blockade, which was also shown to promote lipid storage in white adipose tissue (WAT) and increase liver TG synthesis through mechanisms that are independent from feeding and involves the SNS (Nogueiras *et al*, 2007).

These findings indicate that AgRP-neurons play a role that extends, beyond the regulation of feeding, to the control of peripheral nutrient partitioning. This concept is further substantiated by a recent study showing that Sirt1 invalidation selectively in AgRP-neurons results in a shift in the overall

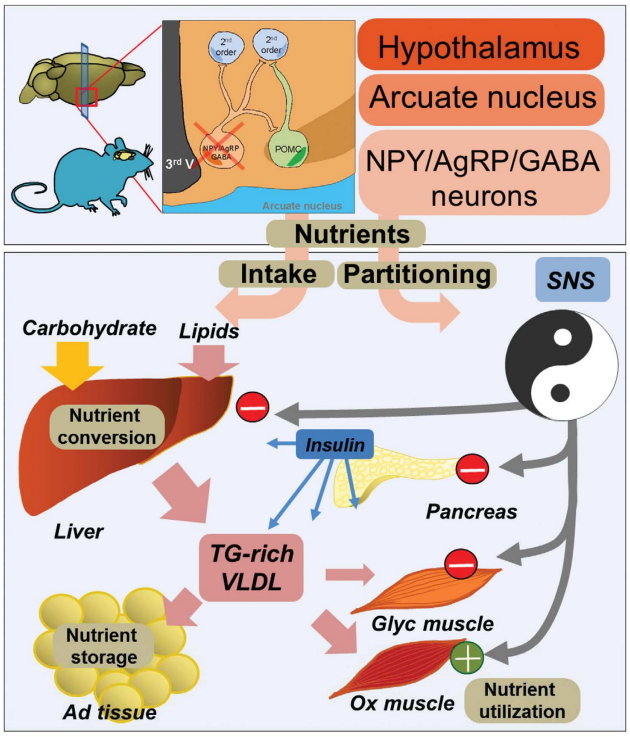

Figure 8 Schematic overview summarizing the consequences of AgRP-neurons depletion on nutrient conversion, storage and utilization. Lack of AgRP-neurons affects food intake and promotes a change in SNS outflow onto peripheral tissues. Whereas SNS outflow is decreased in pancreas, liver and white glycolytic extensor digitorum longum (EDL) muscle, it is increased in oxidative soleus muscle. These changes are associated with increased nutrient conversion, lipid synthesis and export in the liver, and an enhanced preference for lipid substrate in red muscle. Adipose gain results from increased insulin level and sustains adipose expendability and storage capabilities. The overall consequence of increased ratio of fat/carbohydrate oxidation is associated with improved glucose tolerance in mice lacking AgRP-neurons after an HFD.

metabolic profile, the impairment of the metabolic adaptation induced by a fast and a change in ghrelin-induced excitability (Dietrich *et al*, 2010).

Interestingly, several lines of evidence support the existence of MCR-independent pathways by which AgRP-neurons regulate energy balance. For instance, selective activation of AgRP-neurons promotes feeding in Agouti yellow mice (A^y) (Aponte *et al*, 2011), a model in which melanocortin signalling pathway is already tonically inhibited by the ectopic expression of the natural MCR antagonist agouti (Miltenberger *et al*, 1997). Moreover, the modulation of signal transducer and activator of transcription 3 (Stat3) signalling specifically in AgRP-neurons alters locomotor activity and promotes resistance to diet-induced obesity independently of AgRP regulation (Mesaros *et al*, 2008).

Indeed, we found that a $GABA_A$ receptor agonist normalized the RQ profile and reduced adipose tissue in mice lacking AgRP-neurons. These results suggest that GABA may be a crucial signalling molecule by which AgRP-neurons control peripheral nutrient partitioning and are in good agreement with studies implicating GABA release from these neurons in the regulation of feeding (Wu *et al*, 2008, 2009) and metabolic adaptation to an HFD (Tong *et al*, 2008).

Note that in our strategy we ablated AgRP-neurons and therefore all molecules that they make. It is therefore possible that an additional molecule yet to be identified, or some combination of NPY, AgRP and GABA release could be required.

Central determination of nutrient partitioning: what are the consequences for the metabolic syndrome?

One can envision that beside the antagonistic regulation of feeding, both POMC and AgRP-neurons might independently contribute to peripheral nutrient storage, conversion and utilization (carbohydrate versus fat) in a coordinated but not necessarily opposing manner (Figure 8). For instance, selective inactivation of the insulin receptor in AgRP-neurons but not in POMC-neurons results in altered hepatic insulin sensitivity (Konner *et al*, 2007), demonstrating a central dichotomy in the action of insulin that will affect both neuronal population but with different peripheral outcome (Konner *et al*, 2007).

Indeed both population projects to preganglionic structures and the innervation of peripheral tissues by the ANS has distinct organization that can be traced back to pre-autonomic hypothalamic neurons (Kreier *et al*, 2006). Therefore, this central network could be instrumental in the establishment of a metabolic set point by defining, through ANS output, the relative balance between carbohydrate and lipid partitioning. We propose that it is a primary defect in this balance, rather than any direct deleterious action of fat intake *per se*, that would result in the simultaneous impairment of the activity of multiple peripheral organs characteristic of the metabolic syndrome (Elmquist and Marcus, 2003; Buijs and Kreier, 2006; Yamada *et al*, 2008). This model challenges the hypothesis that obesity-related disorders result primarily from a defect in peripheral tissue. For instance, it is believed that the loss of adipose tissue expandability, once reaching a critical mass, results in ectopic deposition of excess lipid in non-adipose organs where accumulation of toxic lipids and pro-inflammatory cytokines will ultimately impair the action of insulin (Reimer *et al*, 2003; Virtue and Vidal-Puig, 2008). Nevertheless, despite obesity AgRP-ablated mice display normal levels of circulating FFA (Supplementary Figure 5) and a significant increase in malic enzyme (a lipogenic marker) in perirenal and subcutaneous adipose tissue of AgRP-ablated compared with naive mice (2.09 ± 0.25 versus 1 ± 0.29, $P < 0.05$, and 2.36 ± 0.53 versus 1 ± 0.25 $P < 0.05$, normalized mRNA level, respectively), suggesting that these mice retained the ability to increase fat mass. Furthermore, despite a similar increase in pro-inflammatory cytokines induced by high-fat feeding (Figure 6; Supplementary Figure 8), AgRP-ablated mice displayed an improvement in glucose tolerance and insulin sensitivity after an HFD. In that regard, AgRP-ablated mice provide a rare example of virtuous adipose expansion that appears to be dissociated from many of the complications associated with obesity, analogous to the way obese *ob/ob* mice with adipose-specific expression of adiponectin are massively obese but remain insulin sensitive (Kim *et al*, 2007). In summary, our study shows that a mere 800 neurons in the ARC of the hypothalamus directly regulate peripheral nutrient fate (partitioning and utilization) through the simultaneous coordination of SNS output onto efferent organs, presumably through GABAergic modulation

of preganglionic structures such as the PVN of the hypothalamus. We thus demonstrate a role for AgRP-neurons, independent from their effects on feeding, in the control of nutrient partitioning and peripheral substrate preference, two core mechanisms linking obesity and obesity-related diseases (Figure 8).

Materials and methods

Animals and experimental design

All animal experiments were performed with approval of the Animal Care Committee at the University of Paris Diderot-Paris 7. Male mice were housed individually in stainless steel cages in a room maintained at 22 ± 3°C with lights on from 0700 to 1900 hours. Food and water were given *ad libitum* unless otherwise. Generation of $Agrp^{DTR/+}$ mice expressing the human DT receptor (DTR; heparin-binding epidermal growth factor receptor) targeted to Agrp locus have been described (Luquet *et al*, 2005). Litters of mice (p2–p6) were injected with DT (75 ng in 20 µl saline) to produce AgRP-ablated mice. Control litters born at the same time were either untreated or injected with saline (naive mice). Food (Safe, Augy, France) was either RCD (3200 kcal/kg protein 21.4%, fat 5.9%, carbohydrates 51.7%) or HFD (4397 kcal/kg protein 17%, fat 22.5%, carbohydrates 42,3%). Feeding responses to peripherally injected ghrelin were measured 4 h after injection of saline or (500 µg/kg i.p.) ghrelin (polypeptides laboratories, France). Feeding efficiency was determined as described in Butler *et al* (2001) by dividing body weight gain (mg) by total calories intake (Kcal) over 4 months for RCD and 2 months for HFD.

Energy expenditure analysis

Mice were analysed for whole energy expenditure, oxygen consumption and carbon dioxide production, RQ (vCO_2/vO_2), food intake and locomotor activity (counts/h) using calorimetric (Labmaster, TSE Systems GmbH, Bad Homburg, Germany). Activity was recorded using infrared light beam-based locomotion monitoring system. Mice were individually housed and acclimated to the chambers for 48 h before experimental measurements.

Data analysis was performed using O_2 consumed (ml/h), CO_2 production (ml/h) and energy expenditure (kcal/h) subsequently expressed as a function of whole LBM as described previously. LBM was acquired using an Echo Medical systems EchoMRI 100 (Whole Body Composition Analyser, EchoMRI, Houston, USA).

Because consistent changes were observed at the onset of the dark cycle, average RQ values were calculated systematically using the same 40-min period at the entry of the dark cycle and analysed using repeated measure ANOVA. Statistical analysis was performed using ANOVA with treatment (NaCl or Ghrelin) and type of mice (naive or AgRP-ablated mice) and their interactions as factors followed by *post hoc* Tukey test.

Atropine and clonidine injection

Mice were food deprived for 5 h before receiving an intraperitoneal injection saline (on day 1) followed by either clonidine (50 nmol/kg) or atropine (26 µmol/kg) (on day 2). Blood was sampled from the caudal vein before and 30-min after injection in order to measure plasma insulin concentration using ultra-sensitive mouse insulin ELISA kit (CRYSTAL CHEM, Downer Grove, IL, USA) according to the manufacturer's protocols.

Oral glucose tolerance test

The oral glucose tolerance test was performed in mice food deprived for 5 h prior to an oral administration of 3 g/kg glucose. Blood was sampled from the tail vein at 0, 5, 15, 30, 60 and 120 min in order to assay glucose concentration (Amenarini glucometer, France).

TG tolerance test

The triglyceride tolerance test was performed in mice food deprived for 3 h prior to an oral administration of olive oil (15 µl/g of body weight) (Kim *et al*, 2007). Blood was collected from the tail vein at 0, 2, 4, 6, 8 h and assayed for TGs, glycerol using the serum TG determination kit (Sigma-Aldrich, France) and FFA using the Nefa-C kit (Sigma-Aldrich). Mice had no access to food during the experiment.

Catecholamine turnover rate determination

Catecholamine turnover was measured on the basis of the decline in tissue NE content after the inhibition of catecholamine biosynthesis with α-methyl-DL-tyrosine methyl ester hydrochloride (α-MPT Sigma-Aldrich, ST Quentin, France) 200 mg/kg i.p, as described previously (Brodie *et al*, 1966).

In the morning, bedding was changed and animals were food deprived for 3 h to insure post-prandial state and injected with α-methyl-DL-p-tyrosine (MPT; a tyrosine hydroxylase inhibitor) to block catecholamine synthesis. Prior to (time = 0) and 3 h after the injection (time = 3 h), animals were sacrificed and tissues were removed. Catecholamine content at time = 0 (NE (0)) was determined on a group of animals receiving a saline injection. Because the concentration of catecholamine in tissues declined exponentially, we could obtain the rate constant of NE efflux (expressed in h-1).

Body temperature measurement

Mice were subdermally implanted with temperature-sensitive probes (IPTT-300, Plexx BV France, France) in the scapular region and allowed to recover for at least 15 days prior to monitoring using telemetric receivers. Diurnal body temperature was recorded during several days of 12 h light/dark cycles at 25°C ambient temperature at specific time point of the day.

Isolation of total RNA and quantitative RT–PCR

For primers sequence see Supplementary data. Total RNA was isolated as described previously (Foretz *et al*, 1999). We retro transcribed 1 µg RNA using Superscript II (Invitrogen). Real-time quantitative (qRT–PCR) analyses were performed with 25 ng cDNA and 250 nM sense and antisense primers (Eurogentec) in a final reaction volume of 25 µl by using qPCR Core Kit (Eurogentec) and the MyiQ real-time PCR detection system (Bio-Rad). Specific primers were designed using Primer Express software (version 1.0, Applied Biosystems) and are shown in Supplementary Table. Relative quantification of each gene was calculated after normalization to Cyclophilin by using the comparative C_t method. Primers sequences are listed in a separate table in Supplementary Materials and methods (see Supplementary Table 4).

Bretazenil treatment

Animals were implanted with subcutaneous Alzet 28-day mini-osmotic pumps delivering 0.25 µl/h (model 2004, Charles River Laboratories, France) of bretazenil (3 mg/ml in saline plus 10% DMSO, cat#B6434 Sigma-Aldrich, France).

Statistical methods

Data were analysed by unpaired Student's *t*-test or, where noted, paired Student's *t*-test or repeated measures ANOVA followed by *post hoc* Tukey test (using Sigmplot 11 software, Systat). Analysis of body temperature was performed using a general linear model. In all tests, a *P*-value < 0.05 was considered significant. All data are presented as mean values ± standard error of the mean or unless specified otherwise.

Supplementary data

Supplementary data are available at *The EMBO Journal* Online (http://www.embojournal.org).

Acknowledgements

This work was supported by young investigator ATIP grant from the CNRS, an equipment grant from the Région Île-de-France, an equipment grant from the University Paris Diderot-Paris 7, a research fellowship from the Société Francophone du Diabète-Lilly and the grant by the 'Agence Nationale de la Recherche' ANR-09-BLAN-0267-02. AJ received a National Merit Scholarship from the French Department of National Education and Research and a research grant from the SFNEP-ANTADIR. RD received a research fellowship from the Région Île-de-France. We express our gratitude to Richard D Palmiter, Susanne E La Fleur, Catherine Postic, Pascal Ferré and Thomas Hnasko for fruitful comments on the manuscript

and Diane Durnam for manuscript editing. We thank Vladimir Veksler for helpful discussion in the design of mitochondrial respiration assay. We thank Justine Bertrand-Michel and François Terce from the IFR50 'Meta Toul' for helpful discussion regarding lipids analysis. We thank Lydia Danglot for helpful input in statistical analysis of body composition data.

Author contributions: AJ-A, RGP, JC, CC designed and performed most of the experiments. RGP and JC performed experiments using indirect calorimetry. AJ-A, RGP, JC and AL carried out *in vivo* experiments and blood chemistry analysis. NK, PDC, MF and FF designed and performed molecular analysis of mRNA expression. RC-P and AP designed and performed experiment on isolated fibres. JD and CR performed the analysis of catecholamine. AJ-A and CM interpreted the data. SL conceptualised, analysed and interpreted all studies and wrote the manuscript.

Conflict of interest

The authors declare that they have no conflict of interest.

References

Ahima RS, Antwi DA (2008) Brain regulation of appetite and satiety. *Endocrinol Metab Clin North Am* **37:** 811–823

Ahren B (2000) Autonomic regulation of islet hormone secretion—implications for health and disease. *Diabetologia* **43:** 393–410

Ahren B, Taborsky G, Porte D (1986) Neuropeptidergic versus cholinergic and adrenergic regulation of islet hormone secretion. *Diabetologia* **29:** 827–836

Aponte Y, Atasoy D, Sternson SM (2011) AGRP neurons are sufficient to orchestrate feeding behavior rapidly and without training. *Nat Neurosci* **14:** 351–355

Bewick GA, Gardiner JV, Dhillo WS, Kent AS, White NE, Webster Z, Ghatei MA, Bloom SR (2005) Post-embryonic ablation of AgRP neurons in mice leads to a lean, hypophagic phenotype. *FASEB J* **19:** 1680–1682

Bouret SG, Draper SJ, Simerly RB (2004) Formation of projection pathways from the arcuate nucleus of the hypothalamus to hypothalamic regions implicated in the neural control of feeding behavior in mice. *J Neurosci* **24:** 2797–2805

Broberger C (2005) Brain regulation of food intake and appetite: molecules and networks. *J Intern Med* **258:** 301–327

Broberger C, Hokfelt T (2001) Hypothalamic and vagal neuropeptide circuitries regulating food intake. *Physiol Behav* **74:** 669–682

Broberger C, Johansen J, Johansson C, Schalling M, Hokfelt T (1998) The neuropeptide Y/agouti gene-related protein (AGRP) brain circuitry in normal, anorectic, and monosodium glutamate-treated mice. *Proc Natl Acad Sci USA* **95:** 15043–15048

Brodie B, Costa E, Dlabec A, Neff N, Snookler H (1966) Application of steady state kinetics to the estimation of synthesis rate and turnover time in tissue catecholamines. *J Pharmacol Exp Ther* **154:** 493–498

Buijs RM, Kreier F (2006) The metabolic syndrome: a brain disease? *J Neuroendocrinol* **18:** 715–716

Butler AA, Kozak LP (2010) A recurring problem with the analysis of energy expenditure in genetic models expressing lean and obese phenotypes. *Diabetes* **59:** 323–329

Butler AA, Marks DL, Fan W, Kuhn CM, Bartolome M, Cone RD (2001) Melanocortin-4 receptor is required for acute homeostatic responses to increased dietary fat. *Nat Neurosci* **4:** 605–611

Cone RD (2005) Anatomy and regulation of the central melanocortin system. *Nat Neurosci* **8:** 571–578

Cowley MA, Cone RD, Enriori P, Louiselle I, Williams SM, Evans AE (2003) Electrophysiological actions of peripheral hormones on melanocortin neurons. *Ann NY Acad Sci* **994:** 175–186

Cowley MA, Pronchuk N, Fan W, Dinulescu DM, Colmers WF, Cone RD (1999) Integration of NPY, AGRP, and melanocortin signals in the hypothalamic paraventricular nucleus: evidence of a cellular basis for the adipostat. *Neuron* **24:** 155–163

Cowley MA, Smart JL, Rubinstein M, Cerdan MG, Diano S, Horvath TL, Cone RD, Low MJ (2001) Leptin activates anorexigenic POMC neurons through a neural network in the arcuate nucleus. *Nature* **411:** 480–484

Dietrich MO, Antunes C, Geliang G, Liu ZW, Borok E, Nie Y, Xu AW, Souza DO, Gao Q, Diano S, Gao XB, Horvath TL (2010) Agrp neurons mediate Sirt1's action on the melanocortin system and energy balance: roles for Sirt1 in neuronal firing and synaptic plasticity. *J Neurosci* **30:** 11815–11825

Dietrich MO, Horvath TL (2009) GABA keeps up an appetite for life. *Cell* **137:** 1177–1179

Eckel RH, Grundy SM, Zimmet PZ (2005) The metabolic syndrome. *Lancet* **365:** 1415–1428

Elmquist JK, Elias CF, Saper CB (1999) From lesions to leptin: hypothalamic control of food intake and body weight. *Neuron* **22:** 221–232

Elmquist JK, Marcus JN (2003) Rethinking the central causes of diabetes. *Nat Med* **9:** 645–647

Foretz M, Guichard C, Ferre P, Foufelle F (1999) Sterol regulatory element binding protein-1c is a major mediator of insulin action on the hepatic expression of glucokinase and lipogenesis-related genes. *Proc Natl Acad Sci USA* **96:** 12737–12742

Gropp E, Shanabrough M, Borok E, Xu AW, Janoschek R, Buch T, Plum L, Balthasar N, Hampel B, Waisman A, Barsh GS, Horvath TL, Bruning JC (2005) Agouti-related peptide-expressing neurons are mandatory for feeding. *Nat Neurosci* **8:** 1289–1291

Haque MS, Minokoshi Y, Hamai M, Iwai M, Horiuchi M, Shimazu T (1999) Role of the sympathetic nervous system and insulin in enhancing glucose uptake in peripheral tissues after intrahypothalamic injection of leptin in rats. *Diabetes* **48:** 1706–1712

Horvath TL, Bechmann I, Naftolin F, Kalra SP, Leranth C (1997) Heterogeneity in the neuropeptide Y-containing neurons of the rat arcuate nucleus: GABAergic and non-GABAergic subpopulations. *Brain Res* **756:** 283–286

Horvath TL, Diano S, Tschop M (2004) Brain circuits regulating energy homeostasis. *Neuroscientist* **10:** 235–246

Horvath TL, Naftolin F, Kalra SP, Leranth C (1992) Neuropeptide-Y innervation of beta-endorphin-containing cells in the rat mediobasal hypothalamus: a light and electron microscopic double immunostaining analysis. *Endocrinology* **131:** 2461–2467

Kim JY, van de Wall E, Laplante M, Azzara A, Trujillo ME, Hofmann SM, Schraw T, Durand JL, Li H, Li G, Jelicks LA, Mehler MF, Hui DY, Deshaies Y, Shulman GI, Schwartz GJ, Scherer PE (2007) Obesity-associated improvements in metabolic profile through expansion of adipose tissue. *J Clin Invest* **117:** 2621–2637

Konner AC, Janoschek R, Plum L, Jordan SD, Rother E, Ma X, Xu C, Enriori P, Hampel B, Barsh GS, Kahn CR, Cowley MA, Ashcroft FM, Bruning JC (2007) Insulin action in AgRP-expressing neurons is required for suppression of hepatic glucose production. *Cell Metab* **5:** 438–449

Krashes MJ, Koda S, Ye C, Rogan SC, Adams AC, Cusher DS, Maratos-Flier E, Roth BL, Lowell BB (2011) Rapid, reversible activation of AgRP neurons drives feeding behavior in mice. *J Clin Invest* **121:** 1424–1428

Kreier F, Kap YS, Mettenleiter TC, van Heijningen C, van der Vliet J, Kalsbeek A, Sauerwein HP, Fliers E, Romijn JA, Buijs RM (2006) Tracing from fat tissue, liver, and pancreas: a neuroanatomical framework for the role of the brain in type 2 diabetes. *Endocrinology* **147:** 1140–1147

Luquet S, Perez FA, Hnasko TS, Palmiter RD (2005) NPY/AgRP neurons are essential for feeding in adult mice but can be ablated in neonates. *Science* **310:** 683–685

Luquet S, Phillips CT, Palmiter RD (2007) NPY/AgRP neurons are not essential for feeding responses to glucoprivation. *Peptides* **28:** 214–225

Mesaros A, Koralov SB, Rother E, Wunderlich FT, Ernst MB, Barsh GS, Rajewsky K, Bruning JC (2008) Activation of Stat3 signaling in AgRP neurons promotes locomotor activity. *Cell Metab* **7:** 236–248

Miltenberger RJ, Mynatt RL, Wilkinson JE, Woychik RP (1997) The role of the agouti gene in the yellow obese syndrome. *J Nutr* **127:** 1902S–1907S

Morton GJ, Cummings DE, Baskin DG, Barsh GS, Schwartz MW (2006) Central nervous system control of food intake and body weight. *Nature* **443:** 289–295

Nilsson I, Johansen JE, Schalling M, Hokfelt T, Fetissov SO (2005) Maturation of the hypothalamic arcuate agouti-related protein system during postnatal development in the mouse. *Brain Res Dev Brain Res* **155:** 147–154

Nogueiras R, Lopez M, Dieguez C (2010) Regulation of lipid metabolism by energy availability: a role for the central nervous system. *Obes Rev* **11:** 185–201

Nogueiras R, Wiedmer P, Perez-Tilve D, Veyrat-Durebex C, Keogh JM, Sutton GM, Pfluger PT, Castaneda TR, Neschen S, Hofmann SM, Howles PN, Morgan DA, Benoit SC, Szanto I, Schrott B, Schurmann A, Joost HG, Hammond C, Hui DY, Woods SC *et al* (2007) The central melanocortin system directly controls peripheral lipid metabolism. *J Clin Invest* **117:** 3475–3488

Nonogaki K (2000) New insights into sympathetic regulation of glucose and fat metabolism. *Diabetologia* **43:** 533–549

Pinto S, Roseberry AG, Liu H, Diano S, Shanabrough M, Cai X, Friedman JM, Horvath TL (2004) Rapid rewiring of arcuate nucleus feeding circuits by leptin. *Science* **304:** 110–115

Porter RK, Brand MD (1993) Body mass dependence of H+ leak in mitochondria and its relevance to metabolic rate. *Nature* **362:** 628–630

Reaven GM (2006) The metabolic syndrome: is this diagnosis necessary? *Am J Clin Nutr* **83:** 1237–1247

Reimer MK, Pacini G, Ahren B (2003) Dose-dependent inhibition by ghrelin of insulin secretion in the mouse. *Endocrinology* **144:** 916–921

Rohner-Jeanrenaud F, Bobbioni E, Ionescu E, Sauter JF, Jeanrenaud B (1983) Central nervous system regulation of insulin secretion. *Adv Metab Disord* **10:** 193–220

Saper CB, Chou TC, Elmquist JK (2002) The need to feed: homeostatic and hedonic control of eating. *Neuron* **36:** 199–211

Schwartz MW, Woods SC, Porte Jr. D, Seeley RJ, Baskin DG (2000) Central nervous system control of food intake. *Nature* **404:** 661–671

Shiuchi T, Haque MS, Okamoto S, Inoue T, Kageyama H, Lee S, Toda C, Suzuki A, Bachman ES, Kim YB, Sakurai T, Yanagisawa M, Shioda S, Imoto K, Minokoshi Y (2009) Hypothalamic orexin stimulates feeding-associated glucose utilization in skeletal muscle via sympathetic nervous system. *Cell Metab* **10:** 466–480

Tong Q, Ye CP, Jones JE, Elmquist JK, Lowell BB (2008) Synaptic release of GABA by AgRP neurons is required for normal regulation of energy balance. *Nat Neurosci* **11:** 998–1000

Virtue S, Vidal-Puig A (2008) It's not how fat you are, it's what you do with it that counts. *PLoS Biol* **6:** e237

Walley AJ, Asher JE, Froguel P (2009) The genetic contribution to non-syndromic human obesity. *Nat Rev Genet* **10:** 431–442

Wu Q, Boyle MP, Palmiter RD (2009) Loss of GABAergic signaling by AgRP neurons to the parabrachial nucleus leads to starvation. *Cell* **137:** 1225–1234

Wu Q, Howell MP, Cowley MA, Palmiter RD (2008) Starvation after AgRP neuron ablation is independent of melanocortin signaling. *Proc Natl Acad Sci USA* **105:** 2687–2692

Wu Q, Palmiter RD (2011) GABAergic signaling by AgRP neurons prevents anorexia via a melanocortin-independent mechanism. *Eur J Pharmacol* **660:** 21–27

Xu AW, Kaelin CB, Morton GJ, Ogimoto K, Stanhope K, Graham J, Baskin DG, Havel P, Schwartz MW, Barsh GS (2005) Effects of hypothalamic neurodegeneration on energy balance. *PLoS Biol* **3:** e415

Yamada T, Oka Y, Katagiri H (2008) Inter-organ metabolic communication involved in energy homeostasis: potential therapeutic targets for obesity and metabolic syndrome. *Pharmacol Ther* **117:** 188–198

